

Received: January 2025, Accepted: April 2025, Published: May 2025  
Digital Object Identifier: <https://doi.org/10.34302/CJEE/DAC01267>

## ORIENTATION OF PHOTOVOLTAIC PANELS USING A PYRAMIDAL SENSOR

Paul NISTOR, Ioan ORHA

Technical University of Cluj-Napoca, Romania

*paul.nistor@ieec.utcluj.ro, ioan.orha@ieec.utcluj.ro*

**Keywords:** sensors, solar panels, renewable energy sources, solar power generation

**Abstract:** The work presents the realization of a solar cell orientation system using a pyramidal sensor. At the base of this system is the pyramidal sensor that captures the luminous flux and transmits it in the form of information to the block responsible for signal processing. The main component within this block is the operational amplifier AO 741, which amplifies the signal before reaching the motor drive block. Within this block we will meet an H-bridge that has the role of changing the direction of the current in the motors, thus resulting in the change of the direction of rotation. In this way, going through all the blocks described, the signal resulting from the pyramid sensor leads to the finality of the movement, namely, the top of the pyramid is oriented towards the sun. When the light flux will fall from a different angle on the sensor, the process will start again, reorienting the pyramidal sensor.

### 1. INTRODUCTION

Concerns about climate change, excessive dependence on fossil fuels and their negative impact on the environment have led humanity to intensify its research on renewable and alternative energies in recent decades [1].

Thus, renewable energy has increasingly become a priority as awareness of environmental issues and the need to diversify our energy sources has grown worldwide. This fact has led to a continuous development in the field of solar, wind, hydroelectric and other forms of renewable energy [2].

This work only concerns the field of solar energy, and the idea of producing such a system comes from an analysis of solar panels and their orientation systems existing on the market.

A general analysis made on the energy efficiency, indicates that the solar panels with an orientation system following the sun are clearly superior to those with a fixed system, registering a significant increase in terms of the level of energy production [3]. Although such a system increases productivity considerably, they present higher costs, mainly due to the need for additional components and more complex software-based technology. Therefore, we decided to implement a simple, reliable and much cheaper system based exclusively on hardware automation, but which would ensure the same performance as a software-based system.

In order to understand how the device works, we will briefly explain the steps taken by the system in the process of orienting the solar panels. It all starts with the pyramidal sensor that captures the light flux and converts it into a signal, which is transmitted to a processing block where the signal will be interpreted. As a result of this interpretation, a command signal is generated which is transmitted to the drive unit of the motors. From this point the motors will be actuated and will lead to the repositioning of the solar panels and the pyramid sensor.

Observing how the system works we can see that the value of this system is found in its simplicity.

## 2. SYSTEM DESCRIPTION

### 2.1. Description of Functional Blocks

The system shown in *fig. 1* follows a perfectly linear course of operation without interference or external adjustments, therefore the device once switched on acquires full autonomy. Even the orientation movement of solar panels based specifically on the concept of action-reaction amplifies this autonomy. The system illustrated in the figure below works exclusively through automatic hardware and in the following paragraphs we will present the electrical components found at the base of each operational block.

The pyramid sensor consists of four photovoltaic cells placed on each face of the pyramid. Photovoltaic cells are grouped in two pairs and connected in parallel, when one pair is illuminated it will provide energy, therefore transmitting a signal while the other pair will remain inactive. We mention the fact that the electrical voltage resulting from the sensor in a direction of travel, depending on how the light flux falls on the pyramid can be positive or negative. If the light flux will fall on both pairs, they will produce energy simultaneously, and due to the fact that they are connected in parallel, they will cancel each other out.

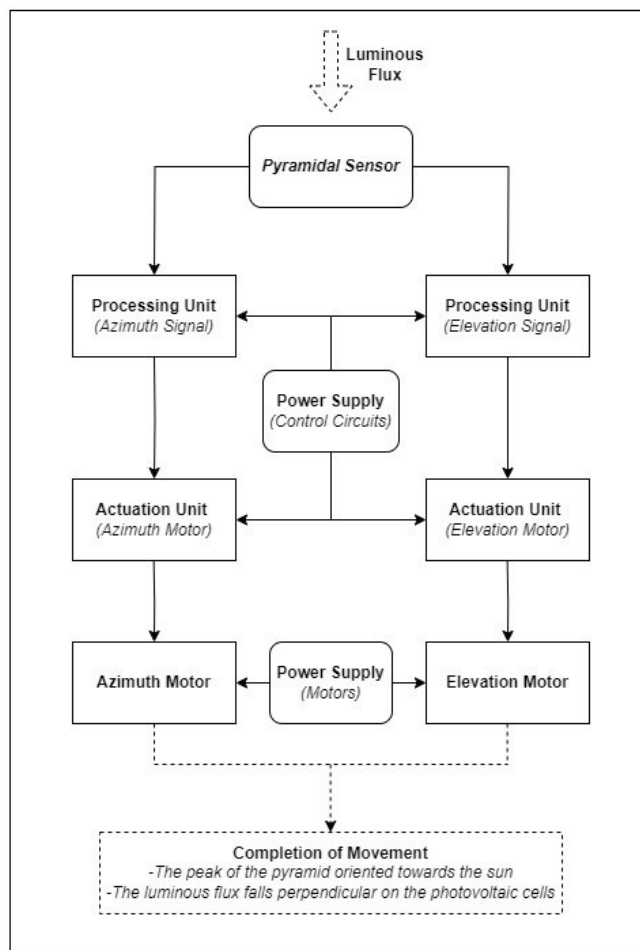


Fig. 1. System structure

It should be noted that this block responsible for capturing the light flux could be made in multiple ways, for example: the geometric shape of the sensor does not have to be a pyramid, it can even be a sphere. The light flux capture element itself does not need to be made with photovoltaic cells, if we wanted to minimize the project we could even use photoresistors.

The reason we used photovoltaic cells is due to the fact that they are built by design to follow the light spectrum that the photovoltaic panels were built for. An added advantage to using solar cells is that they provide easily processed voltages between 0-3V that can be easily filtered by optical and electrical interference.

Regarding the geometric shape used to implement the sensor, we chose the pyramid because it is ideal for capturing the light flux from all four cardinal points thus giving us the necessary signals for elevation and azimuth movement.

The next two blocks present in the system, as the name suggests, deal with the processing of the signal received from the sensor. These circuits are similar, with the only difference that one handles the horizontal movement and the other the vertical one, but the basis of both circuits is the AO741 in the amplifier assembly.

The A0741 circuit has adjustable amplification and can be modified from a semi-adjustable resistor. This feature will control the sensitivity of the orientation circuit and is adjusted at startup under normal lighting conditions.

The output of the operational amplifier attacks a final stage in class B with load distributed in the collectors of the complementary transistors. Transistors being pure class B, they can never both conduct at the same time, having a voltage range at the output of the operational amplifier in which none of the transistors conducts. This creates an interval where the H-bridge is at rest, an event that occurs when opposite faces of the pyramid are equally illuminated. We mention that an RC high-pass filter is placed before the operational amplifier, it has the role of filtering the signal from optical interference.

The next blocks present in the system are those for driving the motors to obtain the two directions, namely azimuth and elevation. These blocks are also identical. Thus each block contains an H-bridge, it is made with relays and is controlled by the previous block. The role of the H-bridge is to change the direction of rotation of the direct current motors, depending on the need to move the photovoltaic panel on which the pyramidal sensor is mounted.

The last two blocks present in the scheme represent the motors that make the movement of the solar panels and the pyramid sensor. These are direct current motors that change their direction of rotation depending on the change of polarity of the supply, they are motors with low consumption and with a simple actuation.

Once all the blocks have been presented, we reach the end of the scheme and also the end of the orientation process of the solar panel. At this point, the top of the pyramidal sensor will be oriented towards the sun and the luminous flux will fall perpendicular to the photovoltaic cells. When the position of the sun changes, the entire system orientation process will be restarted from the first step, going through all the blocks again and reorienting the solar panels.

## 2.2. Electrical Diagram of the System

Through the previously presented blocks, we can understand at least conceptually how the system works. But through the electrical scheme shown in *fig. 2*, we can observe and understand practically how it works.

Although at first look the wiring diagram may seem difficult to understand, it works and is structured exactly like the blocks already explained in the previous paragraphs. In the first part of the electrical diagram, we can observe how the signal reaches the operational amplifier whose amplification is adjusted with the help of potentiometer R3. The output of the amplifier attacks the collectors of the two transistors which can never both conduct at once.

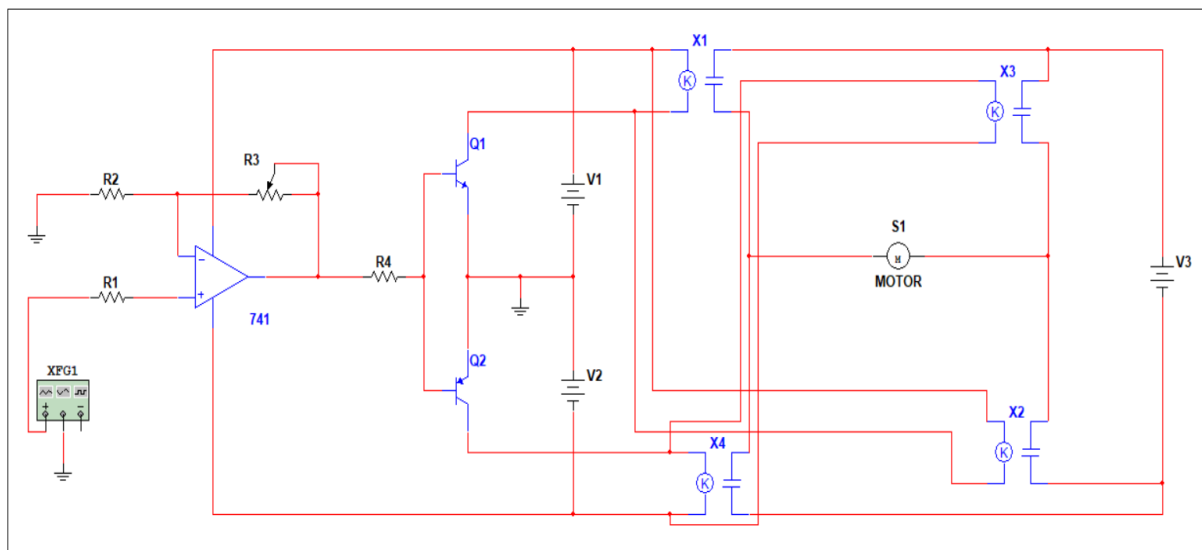


Fig. 2. Electrical diagram of the system

As can be seen in the diagram above, there are four relays that make up two groups. Each transistor is connected to a group of relays, and depending on the need, the required relay group will be activated by one of the transistors. In this way, the polarity of the motor supply is changed, leading to a change in its direction of rotation. Within the system there are two such electrical circuits, one for azimuth movement and the other for elevation movement. We mention the fact that from this electrical diagram itself we can notice the simplicity of the system.

### 3. SIMULATIONS AND RESULTS

In the following, we will present a comparison between a fixed solar panel and a solar panel with an orientation system. Based on these comparisons, it will be possible to see that a solar panel with an orientation system considerably increases the energy produced.

The reason this improvement in energy efficiency occurs is because an orientation system maximizes the solar panel's exposure to solar radiation over the course of a day. This fact is best highlighted on cloudy days or in diffuse light conditions, as the system will adjust the position of the solar panel to optimize the capture of the light flux. In contrast, this adaptability for such conditions is missing in the case of fixed solar panels.

To simulate the energy production of the photovoltaic system, we used the PVGIS (Photovoltaic Geographical Information System) platform [4]. The choice of the PVGIS platform was motivated by the fact that it provides real, long-term climate data, fully validated and used in photovoltaic research at European level.

### 3.1. Characteristics of the photovoltaic module used in the simulations

To perform the energy simulations, we used a monocrystalline photovoltaic module with a nominal power of 150 W, whose technical characteristics and electrical parameters under standard test conditions (STC) are presented in *fig. 3*.

Electrical Characteristics	
	STC
Maximum Power (Pmax)	150Wp
Maximum Power Voltage (Vmpp)	18.0V
Maximum Power Current (Impp)	8.33A
Open Circuit Voltage (Voc)	22.5V
Short Circuit Current (Isc)	9.00A
Power Tolerance(Positive)	5%
Module Efficiency STC	18.66%
Operating Temperature Range	-40°C to +85°C
Maximum System Voltage	1000V
Series Fuse Rating	15A
Temperature Coefficient of Pmax	-0.40 %/°C
Temperature Coefficient of Voc	-0.30 %/°C
Temperature Coefficient of Isc	0.05 % / °C
Nominal Operating Cell Temperature(NOCT)	45±2°C
Mechanical Characteristics	
Cell Type	Monocrystalline 156mm
Cell Number	36 (4x9)
Dimensions (mm)	670x1200x30
Weight(Kgs)	10.00
Front Glass	3.2 mm, High Transmission, Low Iron, Tempered Glass
Frame Type	Anodized Aluminium Alloy
Junction Box Protection Class	IP 67 Rated
Connector Type	MC4
Output Cables	2.5 mm <sup>2</sup> , Length:900 mm

*Fig. 3. Technical characteristics of the 150 W monocrystalline photovoltaic module [5]*

The module has an efficiency at STC of 18.66%, a characteristic value for modern monocrystalline panels, which reflects the ratio between the incident light energy and the useful electrical energy obtained under ideal conditions. These parameters are essential for describing the electrical behavior of the module and serve as input data for modeling the

panel's performance both in a fixed configuration and in a mobile configuration with a tracking system.

Although the efficiency and STC parameters do not directly influence the energy simulation performed through PVGIS, their inclusion is necessary for the complete characterization of the module.

### 3.2. Simulation of the Fixed Photovoltaic System

The performance of the fixed photovoltaic system was evaluated using the PVGIS platform (version 5.3). The simulations were performed for the location of Baia Mare, Romania, characterized by the geographical coordinate latitude  $47.656^{\circ}$  N, longitude  $23.595^{\circ}$  E and an approximate altitude of 240 m. In the analysis, the influence of the local relief was taken into account by activating the automatic horizon calculation option (Use terrain shadows: calculated horizon).

The analyzed system consists of a single photovoltaic panel with a nominal power of 150 W (0.15 kWp), based on crystalline silicon technology. For the performance evaluation, the PVGIS-SARAH3 solar radiation database was used, and the total system losses were estimated at 14%, including losses due to temperature, cables, inverter and other operational factors.

The photovoltaic panel was considered to be mounted on an independent structure (free-standing), with a fixed mounting system. The tilt angle and the orientation towards the south were determined automatically by activating the slope and azimuth optimization option, thus ensuring operating conditions close to the optimal ones for the analyzed location. Based on these settings, the results regarding the energy production and the annual performance of the photovoltaic system were obtained, presented and analyzed in the following section.

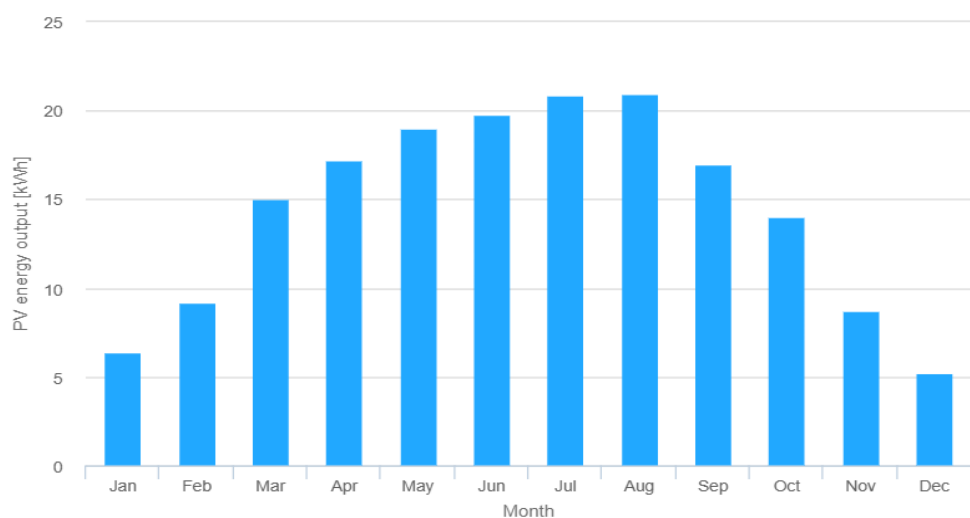
Simulation outputs:	
Slope angle [°]:	37 (opt)
Azimuth angle [°]:	-2 (opt)
Yearly PV energy production [kWh]:	173.38
Yearly in-plane irradiation [kWh/m <sup>2</sup> ]:	1467.38
Year-to-year variability [kWh]:	7.38

Fig. 4. Main results for a fixed PV system

The results obtained in *fig. 4.* show that the analyzed system achieves an annual electricity production of 173.38 kWh, which corresponds to a specific efficiency of approximately 1155 kWh/kWp/year, a value representative for the areas of northern Romania. The annual solar irradiation on the panel plane was estimated at 1467.38 kWh/m<sup>2</sup>, which confirms the existence of an adequate solar potential for the studied location. Following the

automatic optimization process, the optimal tilt angle of the panel was determined at “ $37^\circ$ ”, with an azimuth very close to the southern direction “ $-2^\circ$ ”.

*Fig. 5.* shows the monthly distribution of the electricity produced by the analyzed fixed photovoltaic system. A pronounced seasonal variation in energy production is observed, determined by the change in the level of solar irradiation throughout the year. The maximum production is recorded in the summer months, especially in the period June–August, when the production exceeds 20 kWh, while the minimum values occur in the cold season, reaching approximately 5.25 kWh in December. This behavior is characteristic of fixed-angle photovoltaic systems installed in temperate climate zones and confirms the direct dependence between the energy generated and the availability of the solar resource.



*Fig. 5. Monthly energy output from fix-angle PV system*

### 3.3. Simulation of the Tracking Photovoltaic System

The performance of the tracking PV system (dual-axis tracking) was evaluated using the same simulation platform, PVGIS (version 5.3), to ensure direct comparability with the results obtained for the fixed PV system. The simulations were performed for the same location, keeping the fixed module options active.

The analyzed system consists of a single photovoltaic panel with a nominal power of 150 W (0.15 kWp), based on crystalline silicon technology, identical to that used in the fixed system. The same PVGIS-SARAH3 solar radiation dataset was utilized, while the total system losses were maintained at 14%. Thus, the only difference between the two analyzed configurations is represented by the orientation mechanism of the photovoltaic panel.

In this configuration, the photovoltaic panel was considered mounted on a dual-axis solar tracking system, which allows the continuous orientation of the photovoltaic panel surface in both azimuth and elevation directions, depending on the position of the sun

throughout the day. This mounting strategy ensures a favorable angle of incidence of solar radiation on the panel for a longer period of time compared to a fixed mounting system, leading to an increase in the captured energy.

Simulation outputs	Two axis
Slope angle [°]:	-
Yearly PV energy production [kWh]:	228.48
Yearly in-plane irradiation [kWh/m <sup>2</sup> ]:	1919.53
Year-to-year variability [kWh]:	11.2

Fig. 6. Main results for the tracking PV system

The results obtained in *fig. 6.* indicate an annual electricity production of 228.48 kWh, higher than that obtained in the case of the fixed installation system. This value corresponds to a specific efficiency of approximately 1523 kWh/kWp/year, highlighting the energy advantage of using the solar tracking mechanism. The annual solar irradiation on the panel plane was estimated at 1919.53 kWh/m<sup>2</sup>, a significantly higher value than in the fixed system configuration, as a result of the continuous alignment of the panel with the position of the sun.

The monthly distribution of the electricity produced by the dual-axis tracking photovoltaic system is shown in *fig. 7.* The same seasonal variation characteristic of photovoltaic systems is observed, with maximum production values in the summer period, especially in the months of June–August, when the monthly production reaches approximately 29 kWh, and minimum values in the cold season, with a minimum of approximately 6.5 kWh in December. Compared to the fixed-mount system, the solar tracking configuration leads to an increase in monthly production throughout the year, the difference being more pronounced in periods of high solar irradiation.

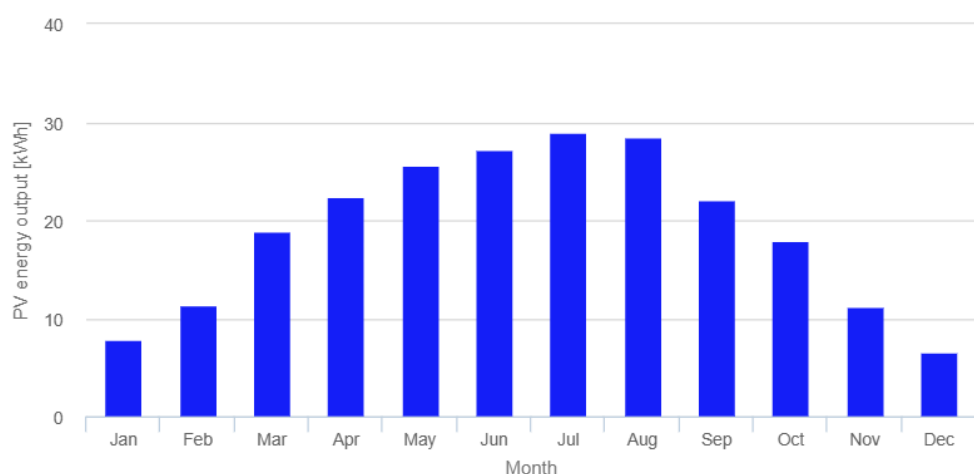


Fig. 7. Monthly energy output from tracking PV system

### 3.4. Comparison of Fixed and Tracking Photovoltaic Systems

Table 1. Monthly energy production comparison between fixed and tracking photovoltaic systems.

Month	Monthly energy production – fixed PV system (kWh)	Monthly energy production – tracking PV system (kWh)	Relative energy gain of tracking system (%)
January	6.38	7.82	22.57
February	9.22	11.44	24.07
March	15.00	18.91	26.07
April	17.22	22.34	29.75
May	18.98	25.58	34.77
June	19.76	27.22	37.76
July	20.84	29.04	39.35
August	20.98	28.49	35.79
September	16.98	22.03	29.74
October	14.01	17.91	27.84
November	8.76	11.14	27.17
December	5.25	6.55	24.76

In Table 1 presents the energy produced by the fixed photovoltaic system and the photovoltaic system equipped with a solar tracking mechanism. The comparison is performed for each month of the year under identical operating conditions. The fourth column presents the relative energy gain of the tracking system, expressed as the percentage increase in energy production compared to the fixed photovoltaic system.

The use of a dual-axis solar tracking system results in a significant increase in energy production throughout the entire year, with relative gains ranging from approximately 22% during the winter months to nearly 40% in summer, the highest improvements being observed between June and July. These results demonstrate that continuous adjustment of the panel orientation allows the system to maintain an optimal incidence angle, leading to enhanced performance, particularly under high solar irradiance conditions.

However, the table above illustrates an ideal case, in which only the gross energy production is considered, without taking into account the energy consumed by the tracking mechanism. In order to provide a more realistic assessment of the efficiency of the mobile system compared to the fixed configuration, the analysis was repeated by deducting the auxiliary energy consumption associated with the tracking system.

### 3.5. Comparison of Fixed and Tracking Photovoltaic Systems Considering the Energy Consumption of the Tracking Mechanism

It is important to specify that within the guidance system, the decision-making part, having a simple structure and being strictly implemented with hardware, generates low energy consumption. In contrast, the execution part, represented by the motors that adjust the position of the solar panel, requires a significant amount of energy. The tracking mechanism is considered at a conceptual level, without a specific motor implementation, and its energy consumption is estimated based on values reported in the literature for small-scale dual-axis tracking systems.

To ensure a conservative and realistic assessment, it was assumed that the auxiliary energy consumption of the tracking mechanism is equal to 5% of the total annual energy production of the tracking PV system. This annual auxiliary energy consumption represents the cumulative energy required for continuous orientation of the panels throughout the year. The estimated annual auxiliary energy consumption was then subtracted from the gross annual energy production obtained from the PVGIS simulations to determine the net energy yield of the tracking system.

Although the auxiliary energy consumption of the tracking mechanism was estimated annually (5% of the total annual energy production), a monthly comparison of net energy was required. Therefore, the annual auxiliary consumption was distributed proportionally over the months, resulting in a uniform 5% reduction in the monthly tracking energy values.

Table 2. Monthly net energy production comparison between fixed and tracking photovoltaic systems, including auxiliary energy consumption

Month	Monthly energy production – fixed PV system (kWh)	Monthly net energy production – tracking PV system (kWh)	Relative net energy gain of tracking system (%)
January	6.38	7.43	16.46
February	9.22	10.87	17.89
March	15.00	17.96	19.73
April	17.22	21.22	23.23
May	18.98	24.30	28.03
June	19.76	25.86	30.86
July	20.84	27.59	32.39
August	20.98	27.07	29.03
September	16.98	20.93	23.26
October	14.01	17.01	21.41
November	8.76	10.58	20.78
December	5.25	6.22	18.47

As shown in Table 2, after accounting for the auxiliary energy consumption of the tracking mechanism, the net annual energy production is reduced to approximately 217.04 kWh. Despite this reduction, the system achieves a specific net yield of about 1447 kWh/kWp/year, which clearly demonstrates the energy advantage of the solar tracking mechanism.

Although the relative energy gain of the tracking system is reduced after accounting for the auxiliary energy consumption, the results demonstrate that a significant net advantage is preserved throughout the entire year. For the small-scale system considered in this study (150 W), the absolute energy gain remains modest, which is expected given the low installed power.

However, it should be noted that the energy consumption of the tracking mechanism does not scale linearly with the installed photovoltaic power. Consequently, the relative benefit of solar tracking systems becomes increasingly relevant for medium and large-scale photovoltaic installations. In the present study, the proposed hardware-based tracking system is demonstrated for a small-scale application, serving as a proof of concept.

In *fig. 8*, we can see our solar panel orientation system. Although this is only a prototype, it is fully functional and successfully demonstrates the possibility of making the current guidance systems more economical and energy efficient using only hardware automation.

Therefore, the comparison between fixed and tracking installations demonstrates that tracking systems achieve a higher energy output, confirming their effectiveness in improving photovoltaic energy production.



*Fig. 8. Actual photograph of the experimental prototype*

#### 4. CONCLUSION

This study presents the design and experimental validation of a photovoltaic panel orientation system implemented exclusively using hardware components. Unlike most commercial solar tracker solutions, which rely on microcontrollers, embedded software and digital signal processing, the proposed system achieves full autonomy through simple analog electronic circuits, resulting in a robust and low-complexity architecture that minimizes cost and potential failure points and removes the need for software programming, continuous calibration and maintenance.

From an economic perspective, the reduction in system complexity translates directly into lower implementation and maintenance costs. The use of widely available analog components, such as operational amplifiers, discrete transistors, and relays, makes the system very attractive for applications requiring low cost. In addition, the absence of digital control units reduces both the initial investment and long-term operating expenses, providing a competitive alternative to commercially available tracking solutions, especially in applications where simplicity and reliability are prioritized.

Another important advantage of the proposed system is the low auxiliary energy consumption at the control level. Unlike many tracking systems available on the market, which require continuous processing and permanently active control logic, the presented solution has low energy consumption at the control circuit level.

The system also shows a high level of flexibility and adaptability. Thanks to its modular design, individual components can be easily replaced or adjusted, including the sensor geometry and the light detection elements. In addition, the adjustable sensitivity of the guidance circuit allows the system to operate effectively under different ambient lighting conditions without requiring a complete redesign. This level of flexibility is rarely found in commercial tracking systems, which are difficult to customize.

In addition to the economic and structural advantages, the proposed solution demonstrates that efficient solar tracking can be achieved without sacrificing performance. Although the absolute energy gain remains modest for small-scale installations, the system serves as a functional proof of concept, validating the feasibility of hardware-based tracking solutions.

In conclusion, the proposed solar tracking system represents a simple, cost-effective and energy-efficient alternative to commercial software-based solutions. By focusing on simplicity, autonomy and low energy consumption, the solution demonstrates that reliable orientation of photovoltaic panels can be achieved with minimal resources, while providing a solid starting point for future improvements and practical applications.

## REFERENCES

- [1] Z. A. Smith, K. D. Taylor, *Renewable and Alternative Energy Resources*, ABC-CLIO, August 2008.
- [2] M. Koussa, A. Cheknane, S. Hadji, M. Haddadi, S. Noureddine, *Measured and modelled improvement in solar energy yield from flat plate photovoltaic systems utilizing different tracking systems and under a range of environmental conditions*, Applied Energy, Vol. 88, No. 5, pp. 1756-1771, May 2011.
- [3] N. A. Kablar, *Renewable Energy: Wind Turbines, Solar Cells, Small Hydroelectric Plants, Biomass, and Geothermal Sources of Energy*, Journal of Energy and Power Engineering, Vol. 13, pp. 162-172, 2019.
- [4] Photovoltaic Geographical Information System (PVGIS). Available: [https://joint-research-centre.ec.europa.eu/photovoltaic-geographical-information-system-pvgis\\_en](https://joint-research-centre.ec.europa.eu/photovoltaic-geographical-information-system-pvgis_en)
- [5] Monocrystalline Solar Panel 150W Datasheet. Available: <https://solarfeeds-media.s3.ca-central-1.amazonaws.com/wp-content/uploads/2022/05/19001109/190520221652937068.pdf>
- [6] J. Rizk, Y. Chaiko, *Solar Tracking System: More Efficient Use of Solar Panels*, World Academy of Science, Engineering and Technology, Vol. 17, 2008.
- [7] F. A. Khalil, M. Asif, S. Anwar, S. Haq, F. Illahi, *Solar Tracking Techniques and Implementation in Photovoltaic Power Plants: a Review*, Proceedings of the Pakistan Academy of Sciences: A. Physical and Computational Sciences, Vol. 54, No. 3, pp. 231–241, 2017.
- [8] P. E. Logan, B. W. Raichle, *Performance Comparison of Fixed, Single, and Dual Axis Tracking Systems for Small Photovoltaic Systems with Measured Direct Beam Fraction*, Department of Technology and Environmental Design, Appalachian State University, NC 28608
- [9] A. Awasthi, A. K. Shukla, M. Manohar, C. Dondariya, K. N. Shukla, D. Porwal, G. Richhariya, *Review on sun tracking technology in solar PV system*, Energy Reports, Vol. 6, pp. 392-405, November 2020.
- [10] A. Saleem, F. Rashid, K. Mehmood, *The Efficiency of Solar PV System*, Proceedings of the 2nd International Multi-Disciplinary Conference, Decembrie 2016.
- [11] H. H. Pourasl, R. V. Barenji, V. M. Khojastehnezhad, *Solar energy status in the world: A comprehensive review*, Energy Reports, Vol. 10, pp. 3474-3493, November 2023.
- [12] P. Sati, A. Kumari, S. Kumar, *Solar energy advancements and their environmental impacts*, Futuristic Trends in Renewable & Sustainable Energy, Vol. 2, March 2023